# Explicit Gibbs free energy equation of state applied to the carbon phase diagram

Laurence E. Fried and W. Michael Howard

*Lawrence Livermore National Laboratory, University of California, Livermore, California 94551*

We provide a simple explicit form for the Gibbs free energy $G(P,T)$ of diamond, graphite, and liquid carbon. The Gibbs free energy function is shown to reproduce the known equation of state properties of carbon up to pressures of 600 GPa (6 MBar) and temperatures of 15 000 K. Recent experiments on graphite melting suggest the presence of a first-order liquid-liquid phase transition at roughly 6 GPa. We show that such a transition is consistent with shock compression data at higher pressures. We reanalyze experiments on the diamond-liquid melting line with our equation of state. Our analysis suggests that the diamond-liquid melting line may have a more positive slope as a function of pressure than previously estimated. A maximum in the diamond melting line is predicted by the model, in agreement with recent *ab initio* simulations.

## I. INTRODUCTION

Carbon is one of the most abundant elements in the universe. Its properties are essential in understanding organic chemistry, biochemistry, and life on earth. The equation of state of elemental carbon under high pressure is of great importance in geology, planetary science, and shock physics.[1] Despite this, the phase diagram and equation of state of carbon under extreme conditions is still not well understood. Diamond is an extremely hard material, so that compressing it substantially under static load is very difficult. The elastic limit of diamond complicates the analysis of shock data.[2] Quantitative data on the melting of diamond under high pressure still do not exist.[3,4]

The study of graphite's high pressure equation of state is also quite difficult. Graphite occurs in a wide variety of multicrystalline forms. The equation of state properties of these forms vary somewhat, complicating the reproducibility of experiments. The melting of graphite, and the location of the graphite-liquid-vapor triple point[5–8] have been the subject of great controversy in the literature. Experiments are complicated by the very high melting temperature of graphite (about 4600 K), finite experimental time scales, and transport effects. Recent *ab initio* simulations may help explain the qualitative properties of graphite melted via laser excitation.[9]

Finally, very little is known about liquid carbon.[10] The very high temperatures involved makes the isolation and study of liquid carbon difficult. What is known about it suggests that it may be a quite unusual material. Recent atomistic simulations suggest a shift from two center to four center bonding as pressure is increased.[11–13] Experiments have shown that the graphite-liquid melting curve has a maximum. Rapoport[14] pointed out in 1967 that such a maximum can be modeled as a mixture of two species. Korunskaya *et al.*[15] explained the melting of graphite in terms of a two-state model of liquid carbon. Ferraz and March[16] proposed a metal–nonmetal phase transition in liquid carbon. More recently van Thiel and Ree proposed a model of liquid carbon based on a mixture of diamondlike and graphitelike liquids.[17–19] They showed that depending on the magnitude of interaction between the liquids, a first-order liquid-liquid transition[20] is possible. Recent theoretical[21,22] and

experimental[23] work has suggested that liquid-liquid phase transitions may occur in common materials, such as water.

Rapid pulsed laser heating of carbon[24,25] has suggested that two different liquid phases of carbon may exist.[26] Togaya recently reported accurate measurements on the melting of graphite under pressure that suggest a first-order liquid-liquid transition.[27] Finally, shock compression data by Shaner *et al.*[28] and other experiments[3] give evidence that the diamond-liquid melting line has positive slope. This result was unexpected and required the re-evaluation of the carbon phase diagram.[29,30]

Several attempts have been made in generating analytical equations of state for carbon that match all of the known data. Gustafson[31] proposed a simple extended Murnaghan[32] equation of state for three phases of carbon. The simple form used for this equation of state, based on a factorization of pressure and thermal effects, is not applicable to states of combined high pressure and temperature.[33] Unfortunately, these states are precisely the ones of most interest in planetary physics and shock physics.

There have also been Mie-Gruneisen equations of state proposed for carbon.[17,18,34,35] The equations of state correctly match shock compression data, unlike Gustafson's form. These equations of state use volume and temperature as the independent variables. In most applications this is somewhat less convenient than using the pressure and temperature as the independent variables. Thermal effects in the equation of state are included by postulating a functional form for the Gruneisen $\gamma = V \partial P/\partial E|_V$. Complicated $\gamma$ functions are necessary to match experimental data.[17,18,34] It is difficult to test the appropriateness of the chosen $\gamma$, since this parameter is rarely measured directly.

In the present paper we propose an equation of state for carbon that attempts to combine the convenience of Gustafson's $(P,T)$ representation with a high degree of accuracy. We find that an appropriately modified Murnaghan equation of state is sufficient to match all known experimental data on carbon. Thermal effects in the equation of state are included through the dependence of the coefficient of thermal expansion on temperature, which can be directly compared to experiment. We provide a closed form for the Gibbs free energy $G(P,T)$ from which all other thermody-

namic properties may be readily derived.

The introduction of a new carbon equation of state is particularly appropriate at the present time. Experiments regarding the compression of diamond,[36] the temperature dependence of the bulk modulus of diamond,[37] the melting line of graphite under pressure,[27,38] and the heat capacity of liquid carbon[39] have appeared in the last several years. *Ab initio* calculations of the equation of state of liquid carbon are also used in the present study.[40] Our equation of state is shown to be consistent with the more recent literature.

The qualitative properties of liquid carbon are of great scientific interest.[26] Our liquid equation of state is shown to match Togaya's recent experiments closely, in addition to high pressure shock compression data. We reanalyze shock experiments on the melting of diamond,[28] and conclude that the experimental boundary on the melting line may be nearly 1000 K higher at 1.4 MBar than previously thought. The fact that a simple equation of state can match independent experiments on liquid carbon over a wide range of pressures (from 1 to 600 GPa) argues for the consistency of the experimental data. Our model predicts a maximum in the diamond melting line at a pressure of roughly 300 GPa, in accord with recent *ab initio* simulations.[40] A possible way to test this prediction experimentally is suggested.

In the next section, we present our form for the Gibbs free energy. The application of the functional form to diamond, graphite, and liquid carbon is considered next in Secs. III, IV, and V. Finally in Sec. VI, we briefly discuss the implications of our model for the phase diagram of carbon.

## II. GIBBS FREE ENERGY EQUATION OF STATE

Our equation of state is based on an explicit functional form for $G(P,T)$. It is more often the case that the pressure of a system is known than its volume. This makes a $(P,T)$ equation of state very convenient in practical application. The form considered here is simple and numerically well-defined for all pressures $0 \leqslant P < \infty$ and temperatures $0 \leqslant T < \infty$. We show below that it yields accurate results in the range $0 \leqslant P \leqslant 600$ GPa and 300 K$\leqslant T \leqslant 15\,000$ K.

We separate the Gibbs free energy into a "reference" portion $[G_0(T)]$ describing properties at $P_0 = 1$ ATM, and an "equation of state" portion describing pressure effects:

$$G(P,T) = G_0(T) + \Delta G(P,T). \quad (1)$$

We first consider $G_0(T)$. Since $G = H - TS$, we have $G_0(T) = H_0(T) - TS_0(T)$. The functions $H_0(T)$ and $S_0(T)$ are conveniently expressed in terms of the constant pressure heat capacity at 1 ATM $C_{p,0}(T)$:

$$H_0(T) = \Delta H_0 + \int_{T_0}^{T} C_{p,0}(T) dT, \quad (2)$$

$$S_0(T) = \Delta S_0 + \int_{T_0}^{T} \frac{C_{p,0}(T)}{T} dT. \quad (3)$$

In the present study we take $T_0 = 298.15$ K, so $\Delta H_0$ is the standard heat of formation and $\Delta S_0$ is the standard entropy. We show below that experimental and calculated heat capacities for graphite and diamond are well represented by the sum of two Einstein oscillators and a linear term:

$$C_{p,0}(T) = \sum_{i=1}^{2} a_i E(\Theta_i/T) + a_3 T, \quad (4)$$

where we use the Einstein form

$$E(x) \equiv \frac{x^2 e^x}{(e^x - 1)^2}. \quad (5)$$

Simple integration yields

$$H_0(T) = \Delta H_0 + \sum_{i=1}^{2} a_i \theta_i \left[ \frac{1}{e^x - 1} \right]_{x_{i0}}^{x_i} + a_3(T^2 - T_0^2)/2, \quad (6)$$

here, $x_i \equiv \Theta_i/T$, and $x_{i0} \equiv \Theta_i/T_0$. We can also analytically determine $S_0(T)$:

$$S_0(T) = \Delta S_0 + \sum_{i=1}^{2} a_i \left[ \frac{x}{e^x - 1} - \ln(1 - e^x) \right]_{x_{i0}}^{x_i} + a_3(T - T_0). \quad (7)$$

This completes the definition of $G_0(T)$. We next consider $\Delta G(P,T)$. Since $dG = V dP - S dT$, $\Delta G(P,T)$ is defined by postulating a form for $V(P,T)$. We then have

$$\Delta G(P,T) = \int_{P_0}^{P} V(P,T) dP. \quad (8)$$

The Murnaghan form uses the relation

$$V(P) = V_0 [n\kappa_0 P + 1]^{-1/n}. \quad (9)$$

This form is derived by assuming that the bulk modulus is a linear function of pressure: $B = B_0 + nP$, where $B_0 = 1/\kappa_0$. In a generalized Murnaghan equation of state, a temperature dependence is added to this form. Gustafson[31] used the form

$$V(P,T) = V_0(T) [n\kappa_0 P + 1]^{-1/n}. \quad (10)$$

As discussed by Plymate and Stout,[33] this form is not accurate for conditions of simultaneously elevated pressures and temperatures.

In the present work, we generalize the Murnaghan form to

$$V(P,T) = V_0 [n\kappa_0 P + f(T)]^{-1/n}. \quad (11)$$

We find below that this form is much more accurate for conditions of elevated pressures and temperatures, such as found in shock experiments. The functional form of $f(T)$ is chosen to reproduce the thermal expansion of the material at zero pressure. We also demand that $f(T) \geqslant 0$ for all $T$, so the equation of state remains well defined for all conditions.

We find that the following form works well for carbon:

$$f(T) = \exp[-n(g(T) - g(T_0))], \quad (12)$$

where

$$g(T) = \alpha_0 T + \alpha_1 \left( T - \frac{T^*}{2} \{\exp[-T/T^*] - 2\}^2 \right). \quad (13)$$

With this equation of state, we find that

TABLE I. Equation-of-state parameters for carbon.

| Phase | $V_0$ (cc/mol) | $B_0$ (GPa) | $n$ | $\alpha_0$ ($10^{-5}$ K$^{-1}$) | $\alpha_1$ ($10^{-5}$ K$^{-1}$) | $T^*$ (K) |
|---|---|---|---|---|---|---|
| Graphite | 5.286 | 33.8 | 8.9 | 2.5 | 1.2 | 1000 |
| Diamond | 3.417 | 441.5 | 3.5 | −0.1 | 1.8 | 450 |
| Liquid 1 | 6.000 | 33.8 | 8.9 | 0.0 | 4.0 | 500 |
| Liquid 2 | 3.950 | 337.8 | 2.0 | −0.1 | 2.4 | 450 |

$$\Delta G(P,T) = \frac{V_0}{(n-1)\kappa_0}[\eta^{n-1} - \eta_0^{n-1}], \qquad (14)$$

where

$$\eta \equiv \frac{V_0}{V} = [n\kappa_0 P + f(T)]^{1/n}, \qquad (15)$$

and $\eta_0 \equiv \eta(T,P_0)$. This completes the definition of $G(P,T)$ used in the present study.

We will now discuss the physical motivation of our choice of $f(T)$. First we note that $f(T_0)=1$, so that a simple Murnaghan isotherm is produced when $T=T_0$. The coefficient of thermal expansion is found to be

$$\alpha \equiv \frac{1}{V}\left.\frac{\partial V}{\partial T}\right|_P = g'(T)\eta^{-n}f(T). \qquad (16)$$

For small expansions and when $T \ll 1/\alpha$, $\eta \approx 1$, and $f(T) \approx 1$. The thermal expansion is thus dominated by $g'(T)$. Below we show that the thermal-expansion coefficient of diamond and graphite are well represented by an initial value, followed by an increase to a final value at high temperature. $g'(T)$ was thus chosen to have the form

$$g'(T) = \alpha_0 + \alpha_1(1 - e^{-T/T^*})^2. \qquad (17)$$

This function increases from $\alpha_0$ to $\alpha_1 + \alpha_0$ as $T$ increases from 0 to $\infty$. The rate of increase is controlled by $T^*$. This form extrapolates to high temperature better than a simple polynomial form, such as that employed by Gustafson.[31] $g(T)$ was then found by integration of $g'(T)$.

## III. DIAMOND

In this section we compare the thermodynamic properties of diamond calculated with our equation of state to experiment. Parameters for the diamond equation of state are listed in Tables I and II. In Fig. 1 we compare the calculated constant heat capacity to experiments.[41] Experimental results for diamond are only available up to 1200 K. A good fit to
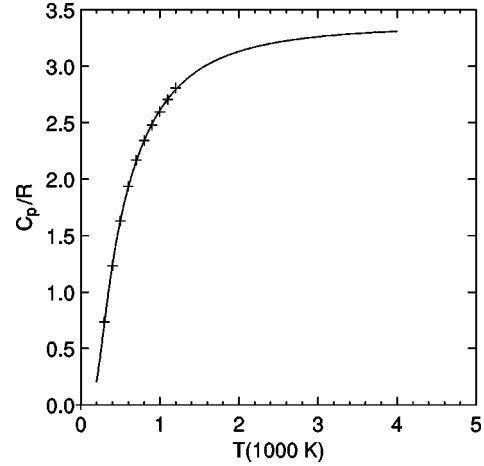


FIG. 1. The calculated constant pressure heat capacity of diamond (solid line) is compared to experiments (Ref. 41) (crosses).

experiment is obtained within this range. As seen in Fig. 1, the Einstein oscillator model provides a reasonable extrapolation to higher temperatures.

Several experiments have been performed on the static compression of diamond. These experiments provide a good test of the choice of bulk modulus, its pressure derivative, and the applicability of the Murnaghan isotherm to diamond. In Fig. 2 we compare experimental isotherm measurements to our model. The model agrees closely with the recent experiments of Fujihisa et al.[36] on pure C$^{12}$ diamond. We also show older experiments by Lynch and Drickamer.[42] These experiments indicate a lower degree of compressibility than more modern experiments. The bulk modulus and pressure derivative $n$ used here are in good agreement with ultrasonic measurements,[43] so we accept the more modern results of Fujihisa et al. Aleksandrov et al.[44] reported the cold compression of diamond up to 70 GPa. Unfortunately, they found that the ruby pressure scale employed was unreliable for pressures above 40 GPa.

We next consider the treatment of thermal effect in the diamond equation of state. Reeber and Wang[45] have proposed a semiempirical quasiharmonic model matching a wide range of thermal expansion data on diamond. The quasiharmonic model provides a physically motivated extrapolation beyond the experimental range of 0–1200 K, while closely matching experiment within this range. In Fig. 3 we compare the thermal-expansion coefficient $\alpha$ predicted by the present model to Reeber and Wang's model. Close agreement is found, validating the postulated form for $f(T)$ and $g(T)$ in Eqs. (12) and (13). We note that we chose $\alpha_0 < 0$, although the expansion coefficient at temperatures less than 100 K has been measured to be very nearly zero.[46] The present model produces a somewhat more accurate fit for $\alpha$

TABLE II. Reference state parameters for carbon.

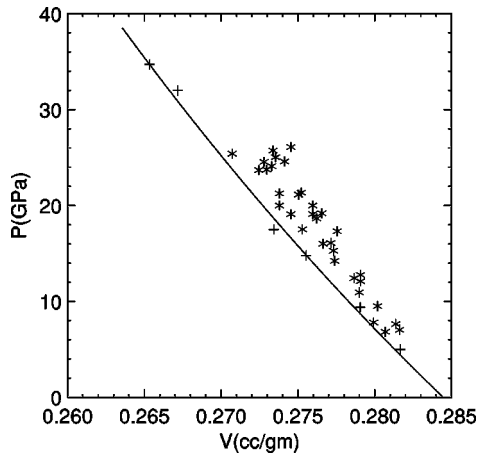| Phase | $\Delta H_0$ (kJ/mol) | $\Delta S_0$ (J/mol K) | $a_1/R$ | $\theta_1$ (K) | $a_2/R$ | $\theta_2$ (K) | $a_3/R$ ($10^{-3}$ K$^{-1}$) |
|---|---|---|---|---|---|---|---|
| Graphite | 0.00 | 5.74 | 1.115 | 597 | 1.789 | 1739 | 0.116 |
| Diamond | 1.82 | 2.70 | 2.594 | 1238 | 0.783 | 3390 | 0.000 |
| Liquid 1 | 65.5 | 3.9 | 4.5 | 1280 | | | |
| Liquid 2 | 112.0 | 25 | 3.5 | 1400 | | | |

FIG. 2. The calculated room-temperature isotherm of diamond (solid line) is compared to experiments of Lynch (Ref. 42) (stars), more recent experiments of Fujihisa (Ref. 36) (crosses).



FIG. 4. The calculated isothermal bulk modulus of diamond at 1 ATM (solid line) is compared to a fit based on elastic constant measurements (Ref. 37) (dashed line).

at temperatures above 298 K, where we intend the equation of state to be used.

Another independent test of the model is found in the dependence of the bulk modulus on temperature at 1 ATM pressure. Zouboulis *et at.*[37] have recently measured the elastic constants of diamond in the range of 300–1600 K. They provide a recommended function fit to their data for the bulk modulus. In Fig. 4 we compare their results to the present equation of state (EOS). We find agreement within the estimated experimental uncertainty of roughly 1%. This indicates that the EOS form is well motivated within this range of temperatures, since no additional parameters were required to match $B(T)$.

Shock compression experiments provide data on the equation of state of diamond at higher pressures than attainable by current static compression experiments. Also, shock compression tests the equation of state under conditions of simultaneously elevated pressure and temperature. In the following calculations, we apply our three phase carbon equation of state to porous samples at differing density before shock compression. This is justified if the shock is sufficiently strong that the material response is plastic. Previous works

have applied this approximation to carbon.[17,18,34,35]

In Fig. 5 we compare the predictions of the present EOS to experiments at differing initial density. Experiments on single-crystal diamond up to 600 GPa were performed by Pavlovskii[47] and Kondo and Ahrens.[2] The points of Kondo and Ahrens at 190 and 217 GPa are shown, along with Pavlovskii's results at 310 and 585 GPa.

Good agreement with experiment is seen, even under the high compressions attained in these experiments. This is strong evidence that the simple Murnaghan form employed here suffices to match the behavior of diamond even under conditions of extreme pressure. The discontinuity in the calculated curve over 560 GPa is caused by the formation of liquid carbon. More discussion of this is given below.

The shock Hugoniot of pressed diamond at an initial density of 3.19 g/cc (Ref. 48) is also shown in Fig. 5. The calculations predict that results should lie on almost the same curve as single crystal diamond. The experimental results agree with this prediction, within the scatter of the data. A much larger dependence on initial density is found in the experiments of Pavlovskii[47] on porous diamond at 1.90 g/cc.
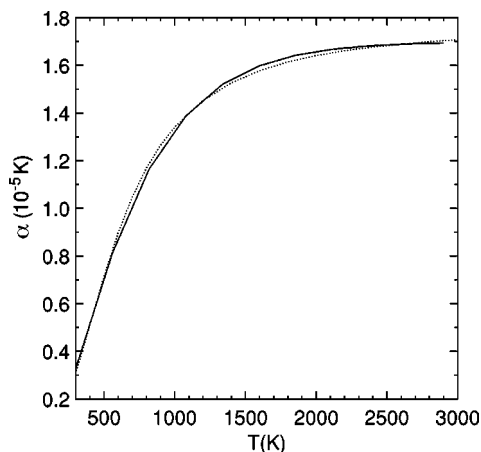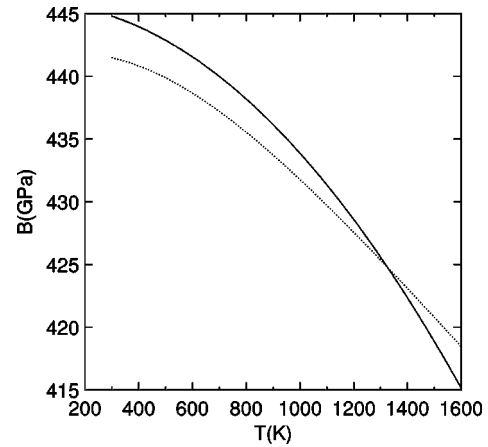


FIG. 3. The calculated volumetric thermal-expansion coefficient of diamond at 1 ATM (solid line) is compared to calculations performed with a quasiharmonic model (Ref. 45) (dotted line).
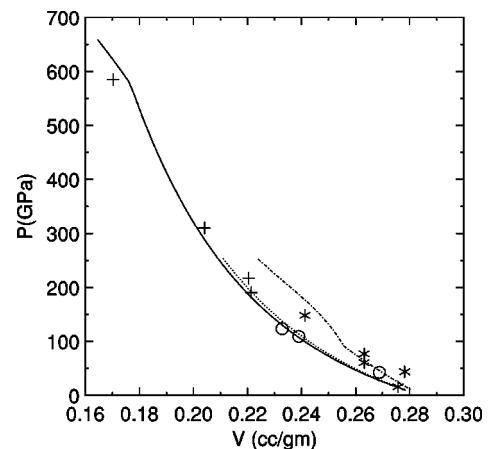


FIG. 5. The calculated shock Hugoniot of diamond at initial densities of 3.51 g/cc (solid line), 3.19 g/cc (dotted line), and 1.90 g/cc (dot-dashed line) is compared to experiments performed at 3.51 g/cc (Refs. 47 and 2) (+), 3.19 g/cc (circle) (Ref. 48), and 1.90 g/cc (Ref. 47) (stars).
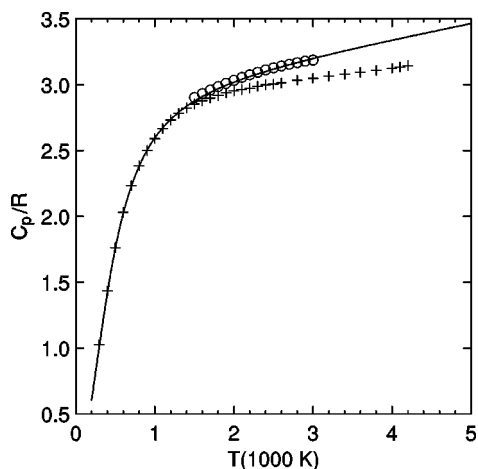
FIG. 6. The calculated constant pressure heat capacity of graphite (solid line) is compared to experiments of Hultgren (Ref. 41) (crosses), and Cezairliyan (Ref. 49) (circles).
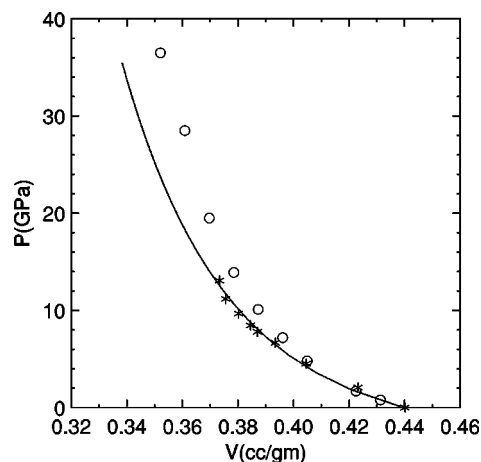


FIG. 7. The calculated room-temperature isotherm of graphite (solid line) is compared to experimental results by Lynch (Ref. 42) (circles) and more recent experiments by Hanfland *et al.* (Ref. 51) (stars).

In this case the shock Hugoniot lies considerably above that of single crystal diamond. The calculations are in good agreement with experiment. The kink in the shock Hugoniot at roughly 80 GPa is caused by a transition to the liquid state. We note that the experimental scatter is somewhat larger for porous diamond than for the other cases. For example, note the points at 15 and 40 GPa. This is typical of experiments on porous materials.[48] The inhomogeneous nature of the material on macroscopic length scales increases experimental scatter.

## IV. GRAPHITE

In this section we compare the thermodynamic properties of graphite calculated with our EOS to experiment. Parameters for the graphite equation of state are listed in Tables I and II. In Fig. 6 we compare the calculated constant heat capacity to experiments.[41,49] The model agrees closely with the values of Hultgren[41] and Cezairliyan[49] up to 1800 K. Above 1800 K Cezairliyan and Hultgren disagree. Values close to Cezairliyan's were chosen as most consistent with other heat-capacity measurements in the JANAF (Ref. 50) thermochemical tables, so we accept Cezairliyan's values here.

We next consider the behavior of graphite under pressure. In Fig. 7 we compare the room-temperature isotherm of graphite to experimental results. As in the case of diamond, Lynch's results[42] seem to be higher in pressure than more modern experiments. We use the values given for $B_0$ and $n$ by Hanfland *et al.* in the present equation of state.[51] Our equation of state shows close agreement with Hanfland's measurements. It is also in good agreement with a calculated all-electron compression curve.[52] Graphite may be prepared in differing polycrystalline morphologies, such as pyrolytic graphite. The thermal expansion of pyrolytic graphite is described in Touloukian and Buyco[53] in the range of 300–3400 K. In Fig. 8 we compare this data to the present equation of state. Good agreement is found.

We next consider the behavior of graphite under shock conditions. Since graphite is metastable to diamond at high pressures, we performed two sets of calculations: one where

the phase of carbon was fixed to be graphite, and the other where the equilibrium phase of carbon was used. In Fig. 9 we compare experiments on pyrolytic graphite[54] to calculations. Calculations in the graphite phase agree well with the experiments up to roughly 35 GPa. Above this pressure, a transition occurs from the graphite phase to the diamond phase. Since kinetic effects are doubtless important in the transition regime,[55,56] the present equilibrium calculations do not match the data in this region. Above 60 GPa the graphite is entirely transformed to diamond, and good agreement is seen between the calculations in the diamond phase and experiment. Experiments on lower density forms of graphite and carbon foams have also been performed.[54,48] We have compared our model to these shock Hugoniots and found that it matches within the spread of the experimental data. The experimental scatter increases with decreasing density, however, so that little new information is gained by the study of these shock Hugoniots.

## V. LIQUID CARBON

Due to the high temperatures involved, the study of liquid carbon is very difficult. Dependences of experimental data
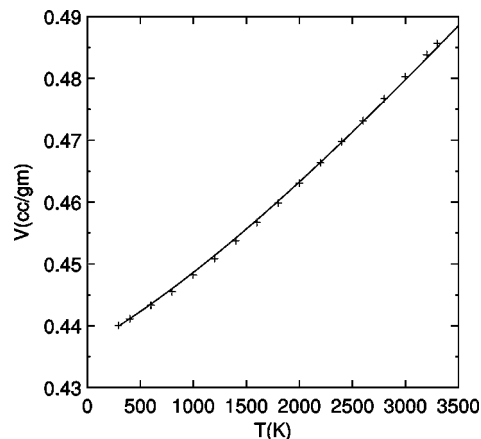


FIG. 8. The calculated thermal expansion of graphite at 1 ATM (solid line) is compared to experimental results for pyrolytic graphite (Ref. 53) (crosses).
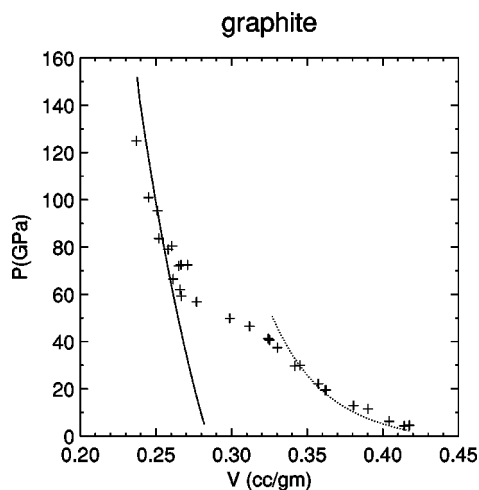
graphite



FIG. 9. The calculated shock Hugoniot of graphite at an initial density of 2.21 g/cc in the diamond phase (solid line) and in the graphite phase (dotted line) is compared to experiments on pyrolytic graphite (Ref. 54) ($+$).
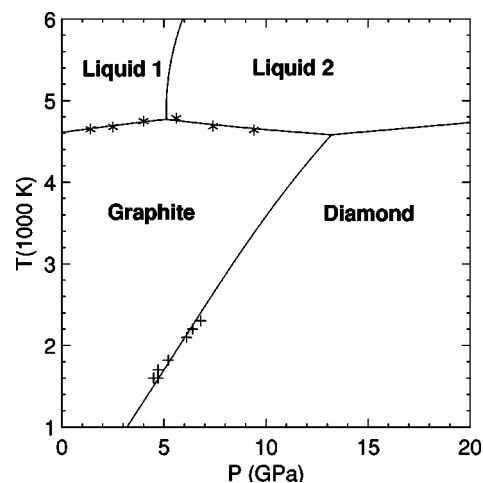


FIG. 10. The calculated phase diagram of carbon is compared to measurements of graphite melting by Togaya (Ref. 27) (stars) and the graphite-diamond phase boundary measured by Bundy *et al.* (Ref. 59) (crosses).

on the time scale of heating have been noted.[7] These difficulties have led to widely varying estimates of the melting temperature of carbon, the location of the solid-liquid-vapor triple point, and other properties. In the present paper, we accept the most recent measurements of Togaya.[27] Previous experiments[57,58] indicated a more pronounced maximum in the graphite melting curve under pressure. Togaya reports the melting temperature of graphite under pressure with high accuracy ($\pm 50$ K). Togaya's low pressure melting data agrees within experimental error with laser heating experiments of Musella *et al.*[38]

Togaya explains the maximum in the melting temperature as a function of pressure in terms of a first-order liquid-liquid phase transition. This is in agreement with previous theoretical work.[14–16,19] We employ the same functional form for the two liquid carbons as that used for diamond and graphite. van Thiel and Ree[19] have suggested that the low-pressure liquid phase (referred to as liquid 1 here) should be graphitelike, while the high-pressure phase (referred to as liquid 2 here) should be diamondlike. The equation of state of the graphitelike and diamondlike phases was derived by scaling of the graphite and diamond equations of state. We use van Thiel and Ree's suggestion as a rough guide in determining appropriate parameters for the equation of state; where there is not enough data to determine the equation of state parameters uniquely, we take parameters from either graphite or diamond.

The constant pressure heat capacity of the liquid 1 phase is set in accordance with a recent experimental estimate of roughly 4 J/K g.[39] The heat capacity of the liquid 2 phase is set to a value appropriate to diamond at high temperatures. A single Einstein oscillator is used, with frequencies appropriate to graphite (liquid 1) and diamond (liquid 2).

In Fig. 10 we show the predicted phase diagram of carbon in the range 0–20 GPa. The graphite melting line shown is composed of two nearly linear segments joining at the liquid-liquid phase transition, as found by Togaya. Note that the slope of the melting line as a function of pressure determines the volume change of melting through the Clausius-Clapyron equation:

$$\frac{\Delta S_m}{\Delta V_m} = \frac{dP}{dT}\bigg|_{\text{melt}}, \tag{18}$$

where $\Delta V_m$ is the volume change upon melting, and $\Delta S_m$ is the entropy change. For the graphite-liquid 1 transition, we have $\Delta V_m > 0$, while for the graphite-liquid 2 transition, we have $\Delta V_m < 0$. Figure 10 also shows that we predict the diamond-graphite phase boundary in good agreement with Bundy *et al.*[59]

The dependence of the enthalpy of melting on pressure, as measured by Togaya, helps to further constrain the liquid equation of state. In Fig. 11 we find that we are able to accurately reproduce Togaya's data on the enthalpy of melting. Togaya's enthalpy data was used to determine $\Delta H_0$ and $\Delta S_0$ for the liquid 1 and liquid 2 states. The enthalpy of melting allows us to obtain quantitative information on $\Delta V_m$, since $\Delta H_m = T \Delta S_m$, which can be related to $\Delta V_m$ through Eq. (18). Although this helps to constrain the liquid parameters, we find that the melting line is fairly insensitive to the choice of $B$ and $n$. For the liquid 1 phase, we simply
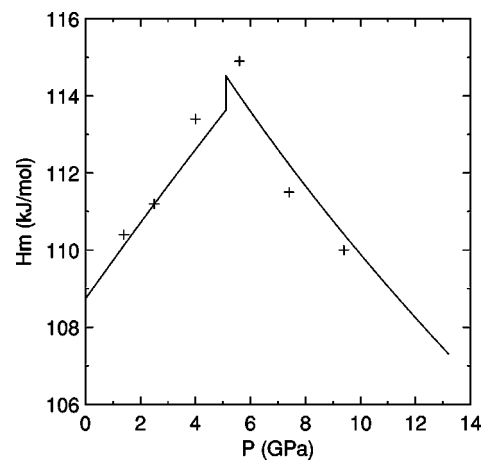


FIG. 11. The calculated enthalpy of melting of graphite is compared to measurements by Togaya (Ref. 27) (crosses).
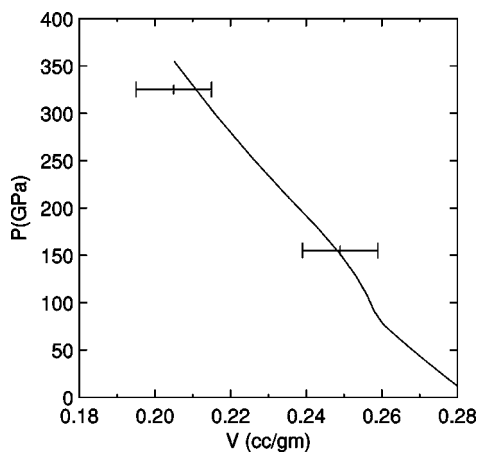
FIG. 12. The measured Hugoniot of graphite (Ref. 61) at 1.85 g/cc shocked into the liquid state (error bars) is compared to the present model (line).



FIG. 13. An isotherm of the liquid 2 phase of the present model at 6000 K (line) is compared to *ab initio* simulation results (Ref. 40) (stars).

use the $B$, $n$, and $\alpha$ appropriate to graphite. Future experiments may help to more uniquely determine these parameters.

For the liquid 2 phase, however, more data is available from shock compression experiments. Sekine[60] has recently made the observation that useful information can be gained on liquid carbon by examining high-pressure shock experiments. Pavlovskii and Drakin[61] report the shock compression of graphite initially at a density of 1.85 g/cc to pressures of 155 and 325 GPa. In Fig. 12 we compare the predictions of our model to this data. The shock Hugoniots of low density forms of carbon have higher error bars than higher density carbon. We have estimated error bars for Pavlovskii and Drakin's experiment by analysis of the shock Hugoniot of pressed graphite at a density of 1.88 g/cc.[48] Our model predicts that the first point is a mixture of diamond and liquid 2, while the second point is entirely liquid 2. These points place an important additional constraint on the equation of state of liquid 2. This helps to determine the bulk modulus $B$ and its pressure derivative $n$. We calculate a temperature of roughly 15 000 K at 325 GPa. This is the highest temperature data considered here. We also note that the shock Hugoniot of porous diamond shown in Fig. 5 contains states containing pure liquid 2 (single-crystal diamond shocked to 600 GPa) and mixtures of liquid 2 and diamond (porous diamond shocked to 150 GPa).

Grumbach and Martin[40] recently performed *ab initio* simulations on several phases of carbon at pressures up to 50 MBar. In particular, they calculated an isotherm of liquid carbon at 6000 K. In Fig. 13 we compare the results of their simulations with the equation of state model for liquid 2 carbon. We find good agreement with the simulations up to pressures of roughly 6 MBar. At pressures above this, Grumbach and Martin find a transition to sixfold coordination in the liquid. This is beyond the scope of the present model, although the model could be extended by adding additional phases of liquid carbon, or by a mixture model.[14] Morris *et al.*[62] report isotherms for liquid carbon at 6000 and 7000 K calculated with tight-binding molecular dynamics. They caution that these isotherms are not fully quantitative. We find that their calculations over 50 GPa are consistent with the liquid 2 model. Under 50 GPa they predict significantly
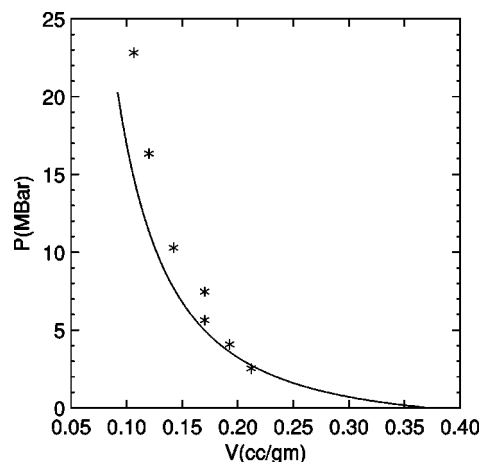
larger volumes than the liquid 2 model. Their predicted volumes are inconsistent with experimental measurements[57,58,27] of a negative slope of the graphite-liquid melting line over 5 GPa.

Shaner *et al.*[28] measured the sound speed of release waves in shocked graphite in the range of 0.8–1.4 MBar. The lack of any decrease in the sound speed with increasing shock pressure indicates that the sample was in a solid phase. Shaner *et al.* calculated $(P,T)$ points along the shock Hugoniot with a simple diamond equation of state. These points have served as a lower bound of the diamond-liquid melting line in several studies.[17,18,30] We have recalculated the $(P,T)$ points with the present equation of state. The results are shown in Fig. 14. We predict that temperatures in the experiment are almost 1000 K higher than those calculated with the model of Shaner *et al.* This means that the experiments place a higher bound on the diamond to liquid melting line than previously thought. Although the calculation of the $(P,T)$ points is not extensively discussed by Shaner *et al.*, we note that the bulk modulus of 5 MBar used is higher than current experimental estimates.[43,36] When used in our model, this bulk modulus lowers the calculated shock temperature by
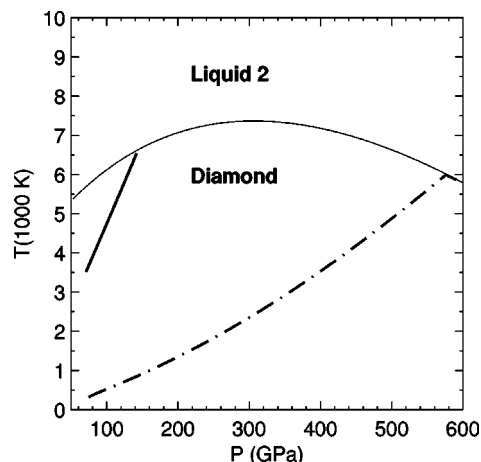


FIG. 14. The calculated melting line of diamond (solid line) and calculations of Shaner's shock experiments (bold line) and the shock Hugoniot of diamond crystal (bold dash-dotted line).

roughly 400 K. The other 600 K probably occurs from the differing treatments of thermal expansion in the two models. Thermal factors are included in the equation of state of Shaner et al.[28] through the choice of the Gruneisen $\gamma$ at standard conditions. We note that the appropriate Gruneisen $\gamma$ ($\gamma = V\alpha B/C_v$) at standard conditions is very uncertain for diamond, given the relatively large error bars on the coefficient of thermal expansion $\alpha$ at room temperature.[46] Galli et al.[12] estimated on the basis of ab initio molecular-dynamics calculations that the melting line of diamond lies between 6500 and 8000 K at pressures of approximately 1 MBar. The current model is 400 K lower than this estimate. We found that the parameter changes necessary to raise the melting line of diamond further (essentially, increasing the bulk modulus of liquid 2 at high pressure) led to results that were not consistent with the shock data in Fig. 12. We conclude that Shaner's experiment at 1.4 MBar comes very close to the diamond-liquid melting line.

In Fig. 14 the diamond melting line has a maximum as a function of pressure at roughly 3.1 MBar and a temperature of 7400 K. Ab initio simulations by Grumbach and Martin[40] led them to predict the existence of a maximum at roughly 3.5 MBar and 8000 K. They attributed the maximum to a transition from a fourfold coordinated liquid to a sixfold coordinated liquid. This is in disagreement with earlier calculations by Young and Grover.[63] In our model, the maximum occurs because the pressure derivative of the bulk modulus is lower for liquid 2 than for diamond. Thus, the relative volume of diamond and liquid 2 changes sign as pressure increases. Since it is not clear whether the transition from fourfold coordination to sixfold coordination is continuous or a first-order phase transition, the relationship between the two mechanisms is not completely clear. We show the calculated $(P,T)$ shock Hugoniot for diamond crystal (density 3.51 g/cc) in Fig. 14. We predict that shocked diamond crystal should begin to melt at a pressure of roughly 5.8 MBar. We also predict that the temperature of diamond crystal shock melting should be slightly less than that of pyrolytic graphite. The melting should be observable in an experiment similar to that of Shaner et al.,[28] and thus could provide direct experimental evidence of the maximum in the diamond melting line.

## VI. CONCLUSION

In the present paper we have presented a simple explicit model for the Gibbs free energy of carbon as a function of pressure and temperature. The model should be applicable to a wide variety of high-pressure applications. We have compared the model to all of the known equation of state properties of graphite and diamond. The model matches the data to within experimental uncertainty. The same model was then applied to liquid carbon. We have shown that Togaya's data on the melting of graphite under pressure[27] can be matched very well with a simple equation of state model, as long as a first-order liquid-liquid transition is assumed.

We have also shown that our model of the liquid 2 phase is consistent with high-pressure shock data, in the sense that the same model can match both types of data. This lends further credence to Togaya's[27] experiments. We then applied our model to the experiments of Shaner et al.[28] determining

the diamond to liquid melting line. We concluded that the melting line is higher in temperature than other equations of state[17,18,35] or recent classical molecular-dynamics simulations[13] have predicted. The model of the liquid 2 phase was shown to match recent ab initio calculations on liquid carbon.[40] This shows that the simulations are consistent with shock compression data on liquid carbon, thus increasing our confidence in the applicability of ab initio techniques to other high-pressure phases[64] such as simple cubic,[64] BC8 (Refs. 65,40) or SC4,[66] where no experimental data exist. Based on matching the available experimental and simulation data, we found that liquid 2 carbon has a zero-pressure bulk modulus close to that of diamond, and that the pressure derivative of the bulk modulus is close to 2.

We have also demonstrated that a simple equation-of-state model of carbon predicts the existence of a maximum in the diamond melting line, in accordance with the latest ab initio simulations.[40] In our model the maximum is caused by the rather low-pressure derivative of the bulk modulus of liquid 2. We have suggested that sound speed measurements of shocked single-crystal diamond may provide experimental confirmation of the melting maximum.

## APPENDIX: FORMULAS FOR OTHER THERMODYNAMIC PROPERTIES

Other thermodynamic properties may be obtained from derivatives of the Gibbs free energy $G(P,T)$. Formulas are given here for completeness. Given the volume $V$, the Gibbs free energy $G(P,T)$, and the enthalpy $H(P,T)$, other thermodynamic potentials can be found through simple addition. $V$ is specified in Eq. (11) and $G(P,T)$ is specified in Eq. (14). $H(P,T)$ is determined by

$$H(P,T) = H_0(T) + \Delta H(P,T), \tag{A1}$$

where

$$\Delta H(P,T) = \frac{V_0}{(n-1)\kappa_0}[\eta^{n-1} - \eta_0^{n-1}]$$
$$+ \frac{V_0 T f'(T)}{n\kappa_0}[\eta^{-1} - \eta_0^{-1}]. \tag{A2}$$

We now determine thermodynamic derivatives. These can be expressed through standard relations in terms of the coef-

ficient of thermal expansion $\alpha$, the isothermal bulk modulus $B$, and the constant heat capacity $C_p$. The relation for $\alpha$ is given in Eq. (16). The bulk modulus is given by

$$B = -V \frac{\partial P}{\partial V}\bigg|_T = \eta^n/\kappa_0. \qquad (A3)$$

The constant pressure heat capacity $C_p(P,T) = C_{p,0}(T) + \Delta C_p(P,T)$. We have

$$\Delta C_p(P,T) = \frac{V_0 f'(T)^2 T}{n^2 \kappa_0}[\eta^{-(n+1)} - \eta_0^{-(n+1)}]$$

$$- \frac{V_0 f''(T)T}{n\kappa_0}[\eta^{-1} - \eta_0^{-1}]. \qquad (A4)$$

[1] H. Hirai and K. Kondo, Science **253**, 772 (1991).

[2] K. Kondo and T.J. Ahrens, Geophys. Res. Lett. **10**, 281 (1983).

[3] M. Togaya, in *Science and Technology of New Diamond*, edited by S. Saito, O. Fukunaga, and M. Yoshikawa (KTK Scientific Publishers/ Terra Scientific Publishing Company, Tokyo, 1990), pp. 369–373.

[4] J.S. Gold, W.A. Bassett, M.S. Weathers, and J.M. Bird, Science **225**, 921 (1984).

[5] C. Ronchi *et al.*, Int. J. Thermophys. **13**, 107 (1992).

[6] M.A. Sheindlin, Int. J. Thermophys. **13**, 95 (1992).

[7] E.I. Asinovskii, A.V. Kirillin, and A.V. Kostanovskii, High Temp. **35**, 704 (1997).

[8] E.I. Asinovskii, A.V. Kirillin, and A.V. Kostanovskii, High Temp. **36**, 716 (1998).

[9] P.L. Silvestrelli and M. Parrinello, J. Appl. Phys. **83**, 2478 (1998).

[10] N. Bloembergen, Nature (London) **356**, 110 (1992).

[11] G. Galli, R.M. Martin, R. Car, and M. Parrinello, Phys. Rev. Lett. **63**, 988 (1989).

[12] G. Galli, R.M. Martin, R. Car, and M. Parrinello, Phys. Rev. B **42**, 7470 (1990).

[13] J.N. Glosli and F.H. Ree, J. Chem. Phys. **110**, 441 (1999).

[14] E. Rapoport, J. Chem. Phys. **46**, 2891 (1967).

[15] I.A. Korunskaya, D.S. Kamenetskaya, and I.L. Aptekar, Fiz. Met. Metalloved **34**, 942 (1972) [Phys. Met. Metallogr. (USSR) **34**, 39 (1972)].

[16] A. Ferraz and N.H. March, Phys. Chem. Liq. **8**, 289 (1979).

[17] M. van Thiel and F.H. Ree, Int. J. Thermophys. **10**, 227 (1989).

[18] M. van Thiel and F.H. Ree, High Press. Res. **10**, 607 (1992).

[19] M. van Thiel and F.H. Ree, Phys. Rev. B **48**, 3591 (1993).

[20] J.N. Glosli and F.H. Ree, Phys. Rev. Lett. **82**, 4659 (1999).

[21] P.H. Poole *et al.*, Phys. Rev. Lett. **73**, 1632 (1994).

[22] P.H. Poole *et al.*, Comput. Mater. Sci. **4**, 373 (1995).

[23] S. Aasland and P.F. McMillan, Nature (London) **369**, 633 (1994).

[24] J. Steinbeck *et al.*, J. Appl. Phys. **58**, 4374 (1985).

[25] A.M. Malvezzi, N. Bloembergen, and C.Y. Huang, Phys. Rev. Lett. **57**, 146 (1986).

[26] J. Steinbeck, G. Dresselhaus, and M.S. Dresselhaus, Int. J. Thermophys. **11**, 789 (1990).

[27] M. Togaya, Phys. Rev. Lett. **79**, 2474 (1997).

[28] J.W. Shaner, J.M. Brown, C.A. Swenson, and R.G. McQueen, J. Phys. (Paris), Colloq. **45**, C8-235 (1984).

[29] F.P. Bundy, Physica A **156**, 169 (1989).

[30] F.P. Bundy *et al.*, Carbon **34**, 141 (1996).

[31] P. Gustafson, Carbon **24**, 169 (1986).

[32] F.D. Murnaghan, Proc. Natl. Acad. Sci. USA **30**, 244 (1944).

[33] T.G. Plymate and J.H. Stout, J. Geophys. Res. **94**, 9477 (1989).

[34] A.B. Averin and A.T. Sapozhnikov, Chem. Phys. Rep. **16**, 255 (1997).

[35] V.V. Dremov and S.I. Samarin, Chem. Phys. Rep. **16**, 249 (1997).

[36] H. Fujihisa *et al.*, Pis'ma Zh. Éksp. Teor. Fiz. **63**, 88 (1996) [JETP Lett. **63**, 83 (1996)].

[37] E.S. Zouboulis, M. Grimsditch, A.K. Ramdas, and S. Rodriguez, Phys. Rev. B **57**, 2889 (1998).

[38] M. Musella, C. Ronchi, M. Brykin, and M. Sheindlin, J. Appl. Phys. **84**, 2530 (1998).

[39] V.N. Korobenko, A.I. Savvatimskii, and R. Cheret, High Temp. **36**, 701 (1998).

[40] M.P. Grumbach and R.M. Martin, Phys. Rev. B **54**, 15 730 (1996).

[41] R. Hultgren *et al.*, *Selected Values of the Thermodynamic Properties of the Elements* (American Society for Metals, Metals Park, Ohio, 1973).

[42] R.W. Lynch and H.G. Drickamer, J. Chem. Phys. **44**, 181 (1966).

[43] H.K. McSkimin and P. Andreatch, Jr., J. Appl. Phys. **43**, 2944 (1972).

[44] I.V. Aleksandrov, A.F. Goncharov, A.N. Zisman, and S.M. Stishov, Zh. Éksp. Teor. Fiz. **66**, 680 (1987) [Sov. Phys. JETP **66**, 384 (1987)].

[45] R.R. Reeber and K. Wang, J. Electron. Mater. **25**, 63 (1996).

[46] K. Haruna, H. Maeta, K. Ohashi, and T. Koike, Jpn. J. Appl. Phys., Part 1 **31**, 2527 (1992).

[47] M.N. Pavlovskii, Fiz. Tverd. Tela (Leningrad) **13**, 893 (1971) [Sov. Phys. Solid State **13**, 741 (1971)].

[48] S. P. Marsh, *LASL Shock Hugoniot Data* (University of California Press, Berkeley, CA, 1980).

[49] A. Cezairliyan, in *Measurement of the Heat Capacity of Graphite in the Range 1500 to 3000 K by a Pulse Heating Method* (The American Society of Mechanical Engineers, New York, New York, 1973), pp. 279–285.

[50] M.W. Chase, Jr. *et al.*, J. Phys. Chem. Ref. Data **14**, 1 (1985).

[51] M. Hanfland, H. Beister, and K. Syassen, Phys. Rev. B **39**, 12 598 (1989).

[52] J.C. Boettger, Phys. Rev. B **55**, 11 202 (1997).

[53] Y. S. Touloukian and E. H. Buyco, *Thermophysical Properties of Matter*, Vol. 13 of *TPRC Data Series* (Plenum, New York, 1977).

[54] W.H. Gust, Phys. Rev. B **22**, 4744 (1980).

[55] D.G. Morris, J. Appl. Phys. **51**, 2059 (1980).

[56] D.J. Erskine and W.J. Nellis, Nature (London) **349**, 317 (1991).

[57] F.P. Bundy, J. Chem. Phys. **38**, 618 (1963).

[58] N.S. Fateeva and L.F. Vereshchagin, Pis'ma Zh. Eksp. Teor. Fiz. **13**, 157 (1971) [JETP Lett. **12**, 109 (1970)].

[59] F.P. Bundy, H.P. Bovenkerk, H.M. Strong, and R.H. Wentorf, Jr., J. Chem. Phys. **35**, 383 (1961).

[60] T. Sekine, Carbon **31**, 227 (1993).

[61] M.N. Pavlovskii and V.P. Drakin, Zh. Éksp. Teor. Fiz., Pis'ma, Red. **4**, 169 (1966) [JETP Lett. **4**, 116 (1966)].

[62] J.R. Morris, C.Z. Wang, and K.M. Ho, Phys. Rev. B **52**, 4138 (1995).

[63] D. A. Young and R. Grover, in *Shock Waves in Condensed Matter 1987*, edited by S.C. Schmidt and N.C. Holmes (North-Holland, Amsterdam, 1988), pp. 131–134.

[64] M.T. Yin and M.L. Cohen, Phys. Rev. Lett. **50**, 2006 (1983).

[65] M.T. Yin, Phys. Rev. B **30**, 1773 (1984).

[66] S. Scandolo, G.L. Chiarotti, and E. Tosatti, Phys. Rev. B **53**, 5051 (1996).